STATE-SPACE FREE VORTEX WAKE FOR FLIGHT MECHANICS: A COMPARATIVE STUDY WITH GLAUERT AND PITT-PETERS INFLOW MODELS

Yusuf BAYRAK
Midde East Technical University & Turkish Aerospace
Ankara, Turkey

Nilay SEZER UZOL
Middle East Technical University
Ankara, Turkey

ABSTRACT

This paper evaluates several rotor inflow models with a focus on the State-Space Free Vortex Wake (SSFVW) model for rotorcraft flight mechanics applications. An articulated rotor based on the UH-60 configuration was implemented using the Helicopter Rotor Simulation (HeRoS) framework in MATLAB/Simulink, employing blade element theory with aerodynamic and inertial coupling. Three inflow models named Glauert, Pitt–Peters, and SSFVW, were assessed through steady-state, trim, and gust response simulations under various flight conditions. Results show that Glauert and Pitt–Peters models capture general aerodynamic trends efficiently, making them well-suited for rapid analysis and control design. In contrast, the SSFVW model provides enhanced fidelity, accurately resolving unsteady wake dynamics and their influence on rotor performance, especially in gusty or maneuvering conditions. Although more computationally intensive, SSFVW demonstrates strong potential for real-time or control applications through further optimization techniques. These findings highlight the trade-offs between fidelity and efficiency and support the ongoing integration of advanced inflow models into rotorcraft simulation frameworks.

NOTATION

*

Symbols

R Rotor radius, m

N_b Number of Blades

Ω Rotor Speed, RPM

c Blade Chord Length, m

λ Inflow Factor

$\lambda_0, \lambda_{1c}, \lambda_{1s}$ Inflow Harmonics

β Flap Angle

$\beta_0, \beta_{1c}, \beta_{1s}$ Flap Harmonics

μ $= \tan^{-1}(V_{vercital}/V_{forward})$ Advance Ratio

α_{disc} $= V_\infty/(\Omega R)$ Rotor Disc Angle of Attack, rad

χ Wake Skew Angle, rad

K_i Glauert Distribution Gain

r Position of the Blade Element or Vortex Particle, m

ψ Azimuth Angle, rad

C_T Thrust Coefficient

C_L Pitch Moment Coefficient

C_M Roll Moment Coefficient

$V_{induced}$ Induced Velocity, m/s

Γ Vortex Strength

ν Kinematic Viscosity of Air, $N \cdot s/m^2$

t Time, s

INTRODUCTION

Helicopter flight simulations require accurate modeling of the rotor aerodynamics. A long-standing challenge is representing the rotor wake and its influence on the rotor disk, called the inflow. The rotor's wake consists of trailing vortices that induce velocity on the rotor, affecting the flow around the rotor.

Simplified models were used historically, but modern technology demands higher fidelity. For example, modern helicopters that have faster maximum velocities or autonomous rotorcrafts are pushing for simulations that remain accurate in complex maneuvers and unconventional flight regimes.

Recent modeling approaches aim to bridge the gap between simple and high-fidelity methods. One promising approach is the state-space free vortex wake model, which aims to combine the accuracy of physics-based wake simulations with the efficiency of a state-space form.

For a helicopter flight dynamics application, an inaccurate wake or inflow model can mispredict the power required, control margins, or stability of the rotorcraft. The most basic analyses often use momentum theory, treating the rotor as an actuator disk that induces a uniform air velocity through it. Glauert's theory was an early application of momentum theory to rotorcraft (Ref. 1). It provided separate formulas for climbing, descending, forward, or hovering conditions. However, it does not develop the solution through time; in other words, it is not a dynamic model, hence the transitions in a time simulation cannot be captured by this model.

By the late 20th century, researchers introduced dynamic inflow models to improve on momentum theory. These models add states to represent the evolution of inflow over time. In one influential example, Pitt and Peters derived a set of first-order differential equations for the induced velocity, yielding a finite-state inflow model (Ref. 2). The Pitt–Peters model includes a uniform inflow state and additional harmonic states corresponding to the first lateral and longitudinal distribution over the disc. Hence, it can capture how inflow builds up or decays with a characteristic time lag. In effect, dynamic inflow models provide a way to predict inflow in a state-space form. This represented a major advancement in computing stability derivatives more realistically (Ref. 2).

Textbooks by Leishman and Johnson detail how such finite-state models improve trim and stability predictions over a simple steady model (Refs. 3, 4). Padfield's work on helicopter flight dynamics also emphasizes that including rotor wake dynamics is important for matching flight test behavior, especially in control response and handling qualities (Ref. 5). In practice, dynamic inflow models have been widely adopted in flight simulators and design tools because they strike a balance between simplicity and accuracy.

Yet, dynamic inflow is still a low-order approximation. It assumes an idealized wake shape and only accounts for its effect on the rotor disc. Real rotor wakes are much more complex as the tip vortices roll up and trail behind, or the wake distorts in transient maneuvering flight, which can create uneven induced flow. Free-vortex wake models were developed to capture this complexity. A free-vortex wake model treats the rotor wake using discrete vortex filaments or particles shed from the blade as it rotates. These models calculate the positions and strengths of vortices over time.

In comprehensive rotorcraft analysis programs such as Flightlab (Ref. 6), free-wake models can predict phenomena like wake skewing in forward flight, tip vortex pairing, and even vortex ring state onset with much higher fidelity than momentum-based models. Johnson (Ref. 4) notes that free-wake methods represent the state-of-the-art in rotor aerodynamics modeling, minimizing theoretical approximations by directly simulating the wake physics. The payoff is more accurate performance and load predictions, but the cost is heavy computation and complexity.

Historically, using a full free-vortex wake in real-time flight dynamics simulation or in linear control analysis was impractical. Free-wake codes might take minutes or hours to run a maneuver, whereas simulators require faster than real-time calculations. Moreover, a free wake is not naturally in a state-space form as it is a set of moving points or filaments in space, which complicates getting system matrices or doing stability analyses. This is where the state-space free vortex wake (SSFVW) modeling approach comes in. The idea is to reformulate the wake model into a set of state equations.

Roberto Celi (2005) applied the method of lines to the rotor wake equations, creating a state-space approximation of a free-vortex wake (Ref. 7). Essentially, the continuous vortex wake is discretized into a finite set of ordinary differential equations. This was a significant development since it opened the door to including high-fidelity wake effects in flight simulations and to linearize the model for control design.

Following Celi's work, further research explored and refined state-space wake models. Hidalgo (2014) carried out a comprehensive assessment of a state-space free wake model for rotorcraft flight mechanics (Ref. 8). More recently, Saetti and Horn (2022) implemented a state-space free-vortex wake model in a rotor simulation and performed a full linearization of the coupled system (Ref. 9).

To contribute to this ongoing development, a rotor model based on the UH-60 configuration has been implemented using the blade element method in MATLAB/Simulink. The framework, named Helicopter Rotor Simulation (HeRoS), incorporates both aerodynamic and inertial force calculations along the blade span and allows flap and lead-lag degrees of freedom. This model has been introduced in (Ref. 10).

Although prior studies have validated SSFVW models in academic settings, their direct comparison with classical models under unified rotor configurations remains limited. The goal of this study is to compare the SSFVW model with widely used inflow models like Glauert and Pitt-Peters under various flight conditions. The performance of these models is analyzed in terms of their impact on steady-state forces and moments, trim conditions, and gust responses.

METHODOLOGY

This section presents the mathematical modeling techniques and inflow models used in the simulation. Three different inflow models were implemented and compared under a common simulation framework. The details of the simulation environment and each inflow model are provided below.

Table 1. Rotor Model Parameters Used in the Simulation.

Parameter	Value
Number of blades N_b	4
Rotor radius R	8.2 m
Blade mass	128 kg
Hinge offset	0.37 m
Rotor speed Ω	258 RPM
Blade airfoil	NACA 0012
Blade chord c	0.53 m
Twist distribution	Linear (10° at root to –3° at tip)
Flap Spring Constant	0 N $\cdot m/rad$
Lag Damper Constant	27116 N $\cdot m \cdot s/rad$

Simulation Framework

The simulations were performed using a modular helicopter rotor model developed in MATLAB/Simulink, called HeRoS (Ref. 10). This framework calculates the aerodynamic and inertial forces on multiple spanwise segments of the blade. The blades are assumed to be rigid, but they can flap and lead-lag with first-order hinge dynamics, including damping and stiffness, as defined in 1. Blade element theory is used to compute local forces, and induced velocities are applied using the selected inflow model.

The rotor is based on the UH-60 Black Hawk configuration, same as Flightlab (Ref. 6), and its parameters are listed in Table 1.

Glauert Inflow Model

The Glauert model is an extension of uniform inflow theory. It assumes that the rotor acts as an actuator disk and uses momentum theory to estimate the induced velocity. In momentum theory, the induced velocity is computed from the energy balance. This computation is an iterative solution of Eq. 1.

$$\lambda = \mu \tan(\alpha_{disc}) + \frac{\lambda_{hover}}{\sqrt{\mu^2+\lambda^2}} + \lambda_{vercital}\cos(\alpha_{disc}) \quad (1)$$

In forward flight, an empirical expression is used to account for the wake skew angle.

$$K_i = \tan(\chi/2) \quad (2)$$

$$\lambda_0 = \lambda \quad (3)$$

$$\lambda_{1c} = K_i\lambda \quad (4)$$

The radial distribution of the induced velocity is expressed as:

$$\lambda_{element} = \lambda_0 + \lambda_{1c}\frac{r}{R}\cos(\psi) \quad (5)$$

Glauert's model provides separate expressions for climb, descent, and forward flight regimes, but it does not evolve through time and does not include any dynamic states (Ref. 1). Hence, the solutions are according to the flight conditions at the time instant; in other words, the information about inflow from the past will not be used.

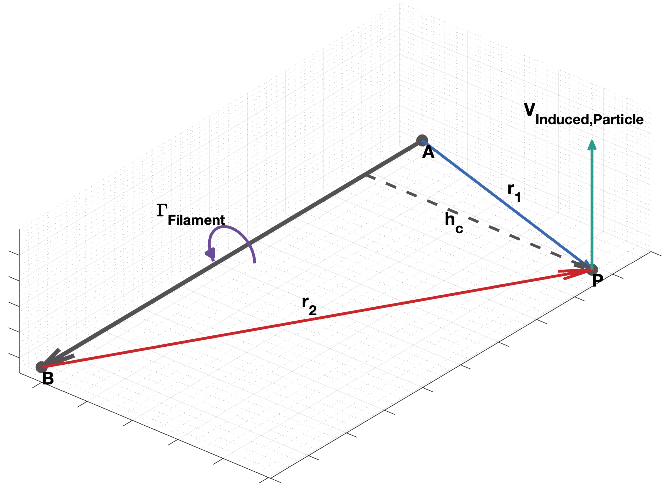

Figure 1. Vortex Filament

Pitt–Peters Dynamic Inflow Model

The Pitt–Peters model introduces a low-order dynamic inflow formulation. The model consists of three states representing the uniform, longitudinal, and lateral components of the inflow. These states evolve based on the rotor thrust and moment coefficients.

The state-space form is given by:

$$\begin{bmatrix}\dot{\lambda}_0\\ \dot{\lambda}_{1c}\\ \dot{\lambda}_{1s}\end{bmatrix} = \Omega\hat{M}^{-1}\left(\begin{bmatrix}C_T\\ C_L\\ C_M\end{bmatrix} - \hat{V}\left(\hat{L}^{-1}\begin{bmatrix}\lambda_0\\ \lambda_{1c}\\ \lambda_{1s}\end{bmatrix}\right)\right) \quad (6)$$

where,

The inflow at each blade element is reconstructed as:

$$\lambda_{\text{element}} = \lambda_0 + \lambda_{1c}\frac{r}{R}\cos(\psi) + \lambda_{1s}\frac{r}{R}\sin(\psi) \quad (7)$$

This model enables time-domain analysis of induced flow and allows linearization for stability studies (Ref. 2).

State-Space Free Vortex Wake Model

The state-space free vortex wake (SSFVW) model is a high-fidelity inflow model derived from a physics-based representation of the free vortex wake. Only tip vortices are considered and they followed for 0.5 seconds which corresponds slightly more than 2 revolutions of rotor. A new vortex particle is shed at each time step, and its position and circulation are tracked as state variables.

The particle dynamics are modeled by:

$$\dot{r} = -A_\zeta r - V_\infty + \sum V_{\text{induced},k} \quad (8)$$

$$\dot{\Gamma} = A_\zeta \Gamma \quad (9)$$

where A_ζ is a finite difference matrix defined by Celi (Ref. 7).

The induced velocity at a point is calculated using the Biot–Savart law as done in Eq. 10 and visualized in 1.

$$V_{\text{induced},P} = \frac{\Gamma}{4\pi}K_{\text{core}}\frac{r_1\times r_2}{\|r_1\times r_2\|^2}\left(\frac{l_{AB}\cdot r_1}{\|r_1\|} - \frac{l_{AB}\cdot r_2}{\|r_2\|}\right) \quad (10)$$

where l_{ab} is the vector from point A to B.

To prevent singularities at short distances, a vortex core correction model called the Vatistas core model is used (Ref. 11), which smooths the vortex core using a parameterized radius and decay exponent.

In addition, Lamb–Oseen vortex growth is implemented to allow the core radius to grow with time, defined as:

$$r_c(t) = \sqrt{r_{c,0}^2 + 4\nu t} \tag{11}$$

where $r_{c,0}$ is the core size for a freshly shed vortex element taken as 5% of the radius.

This model provides a detailed evolution of the rotor wake and its effect on the flow around the rotor, suitable for transient analyses and linearization (Refs. 7,9).

RESULTS

There are three main kinds of analysis done to compare the inflow methods mentioned: steady-state, trim, and simulation analysis

Trim Analyses

In the trim analyses, the objective is to find the equilibrium condition where the rotor generates a predefined thrust of approximately 60710 N without producing any net rolling or pitching moments. This condition is achieved while the rotor is subjected to different combinations of horizontal and vertical wind velocities, representing a sweep across various flight conditions.

The trimming process involves iteratively adjusting the collective and cyclic control inputs until the target thrust and moment conditions are satisfied within specified tolerances, by iterating on the controls to drive force and moment errors to near zero.

In the first application of this analysis, the trimming results are validated against data obtained from FlightLab (Ref. 6), a widely used and extensively validated rotorcraft modeling and simulation software. FlightLab's credibility and established accuracy in rotorcraft aerodynamics provide a strong reference point for assessing the fidelity of the developed inflow models.

The first analysis case is for a forward flight from hover to 50 m/s. The trim controls are compared in the Figure 2.

According to the Figure 2, as forward velocity increases, the collective pitch generally decreases for all models to compensate for the decreasing inflow. The SSFVW model consistently demands higher collective input than the others. It predicts more induced losses or a less efficient inflow, requiring greater blade pitch to generate the same thrust. FlightLab's vortex wake model matches the SSFVW model for forward flight conditions ranging from 10 to 35 m/s. Although FlightLab predicts less before this interval, it predicts more collective input after the interval. At high forward speeds, the accuracy of the SSFVW model decreases due to the rapid convection of vortex particles beyond the near-wake region, limiting

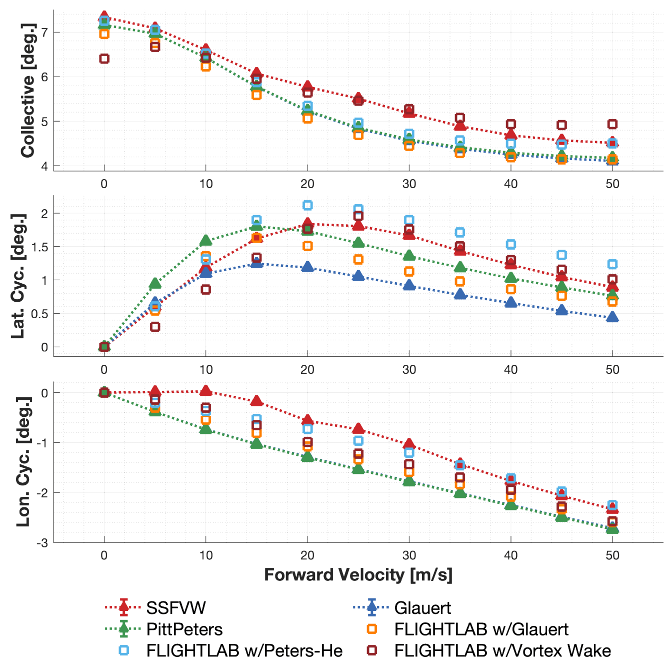

Figure 2. Trim Controls for Forward Flight

its ability to represent the full wake structure. In contrast, FlightLab's Scully periodic vortex wake model, while more consistent at higher speeds, is known to underpredict induced inflow in hover, making it less reliable in that regime.

In terms of cyclic inputs, both lateral and longitudinal cyclic requirements increase with speed, showing the effect of the asymmetry in lift and pitching moments across the rotor disc. In lateral cyclic, all the models match with the expectations and behave in a similar pattern with different magnitudes or peaks. A similar trend is observed in the longitudinal cyclic input. Although all models exhibit comparable slopes, the SSFVW model underpredicts the required longitudinal cyclic at low forward speeds. This discrepancy arises from the dominance of inflow contributions near the rotor hub, where the SSFVW model lacks sufficient resolution or representation of near-hub vorticity effects.

Furthermore, the Figure 2 shows how the HeRoS and FlightLab results match for different inflow models implemented on them, which can be considered as proof of validation of HeRoS.

In climb and descent, a similar behavior is observed. In Figure 3, a case to compare the models for climb and descent is shown. In this analysis, all the models are trimmed with 35 m/s forward velocity, and the vertical wind component is swept from 5 to -5 m/s. For all the control inputs, an unsymmetrical behavior for downward velocity is observed in Glauert since it has a different analytical solution for the climb and descent conditions; hence, the slope of the control inputs is different for these cases. On the other hand, the Pitt-Peters and SSFVW models are quite similar except for the lateral cyclic, which is expected since the estimation of inplane forces, dominant in the lateral axis, is different for both models.

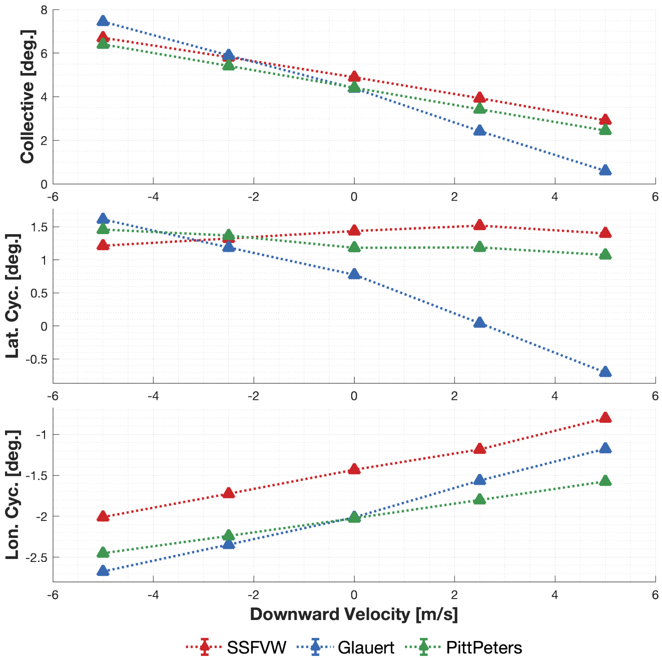

Figure 3. Trim Controls for Climb and Descent with 35 m/s Forward Velocity

In terms of inflow distributions at trim, the Figures 4, 5, 6 shos the distribution across the disc for hover, and Figures 7, 8, 9 for forward flight are obtained. Note that these figures have the same color bar limits set, so they did not repeat after the first one.

In hover, Figures 4, 5, and 6, the results from 3-State Pitt-Peters and Glauert inflow models are quite similar. On the other hand, for the same condition at trim, the SSFVW model provides a much richer inflow distribution across the disc. In hover, the radial distribution dominates, and the inflow is reduced at tips and reaches maximum in an inner section because of the wake contraction.

In forward flight, Figures 7, 8, 9, the behavior of the Pitt-Peters and Glauert inflow models is similar, but their skewness is not the same, as the Pitt-Peters results in a more skewed distribution. Furthermore, SSFVW has a similar skewness with some radial changes.

One of the key advantages of the SSFVW model is its ability to capture the detailed wake geometry and its influence on the surrounding flow field, which cannot be resolved by traditional analytical inflow models. Figures 10 and 11 illustrate the wake structure at hover and forward flight, respectively.

In hover (Figure 10), the wake exhibits strong contraction due to the concentrated vortex core near the rotor hub and the induced axial flow. In forward flight (Figure 11), distinct vortex roll-ups are observed, especially on the advancing side of the disc, where blade loading is higher. These roll-ups are less pronounced on the retreating side due to reduced dynamic pressure.

Figures 12 through 15 present the induced velocity field around the rotor under different flight conditions. In hover (Figure 12), the wake primarily affects the region between

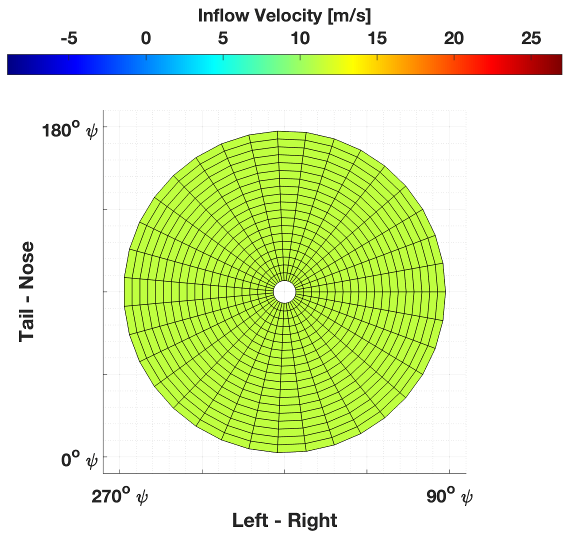

Figure 4. Inflow Distribution with Glauert Model at Hover Trim

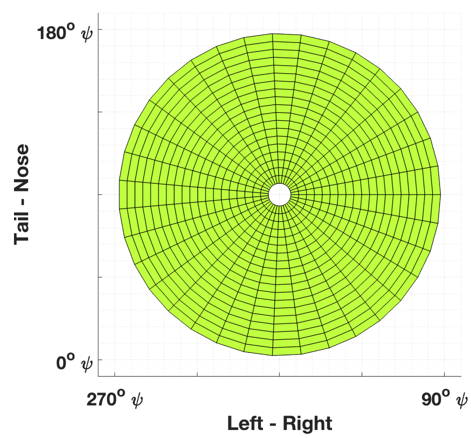

Figure 5. Inflow Distribution with Pitt-Peters Model at Hover Trim

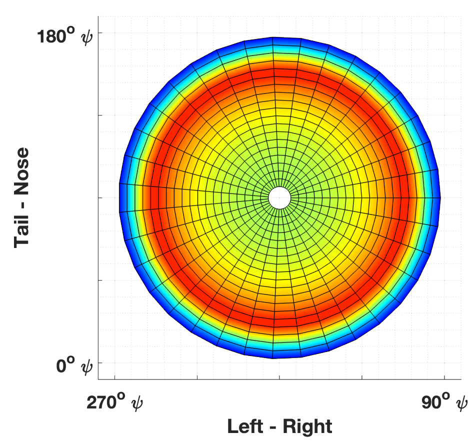

Figure 6. Inflow Distribution with SSFVW Model at Hover Trim

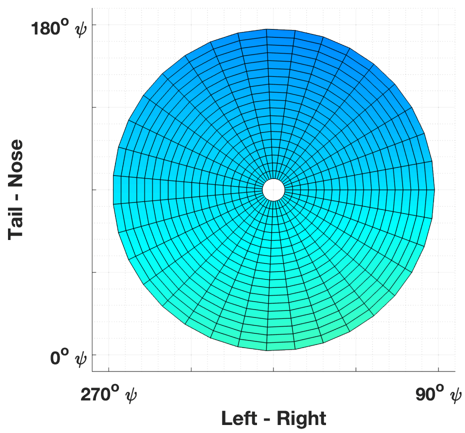

Figure 7. Inflow Distribution with Glauert Model at 35 m/s Forward Flight Trim

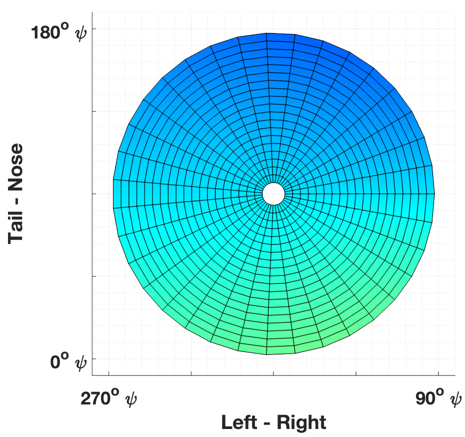

Figure 8. Inflow Distribution with Pitt-Peters Model at 35 m/s Forward Flight Trim

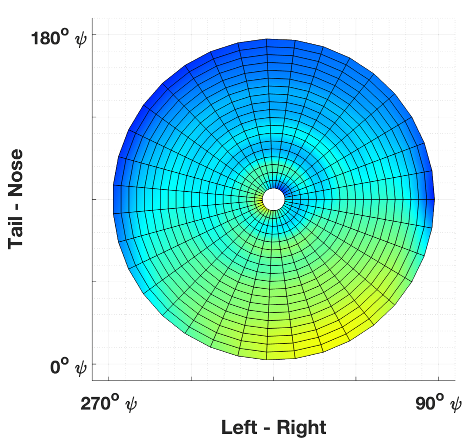

Figure 9. Inflow Distribution with SSFVW Model at 35 m/s Forward Flight Trim

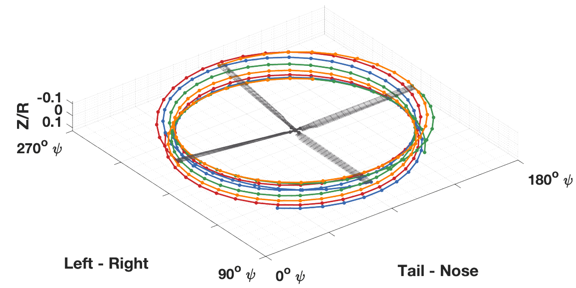

Figure 10. Wake Structure with SSFVW Model at Hover Trim

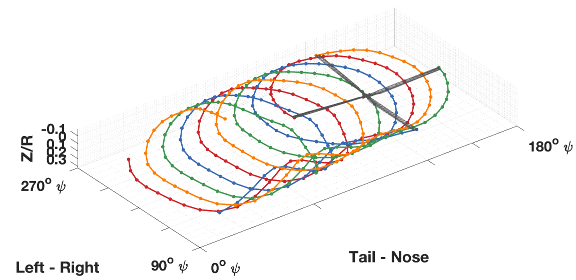

Figure 11. Wake Structure with SSFVW Model at 35 m/s Forward Flight Trim

50% and 90% of the rotor radius and maintains an approximately symmetric and uniform distribution in the azimuthal direction.

The Figures 12, 13, 14, and 15 show how the wake affects the flow around the rotor in different flight conditions. In hover, like in Figure 12, the wake is more effective between 90% and 50% of the rotor radius and maintains an approximately symmetric and uniform distribution in the azimuthal direction.

In forward flight (Figure 13), the wake is convected rapidly downstream, and the wake particles are quickly washed off to the back of the disc. The effect at the 180° ψ is very low and near zero, in contrast to the back side of the disc as seen. his asymmetry indicates increased interaction between the rotor wake and the aft fuselage in a full aircraft configuration.

In climb and descent, the wake is influenced by the vertical component of the freestream. As shown in Figures 14 and 15, the wake convects along the flow direction. In climb (Figure

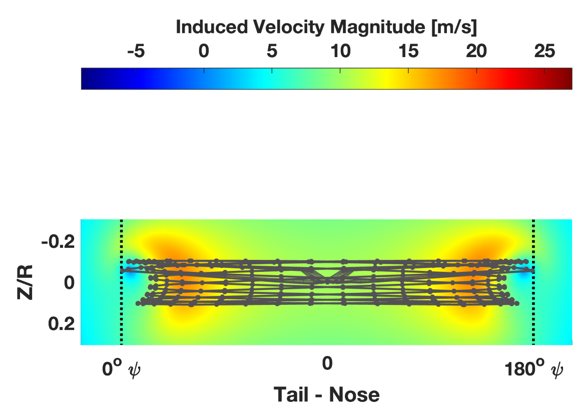

Figure 12. Induced Flow Around Rotor with SSFVW Model at Hover Trim

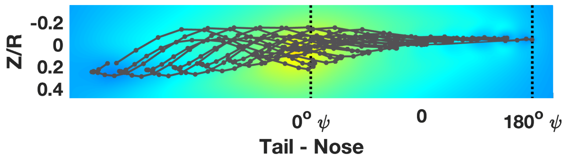

Figure 13. Wake Structure with SSFVW Model at 35 m/s Forward Flight Trim

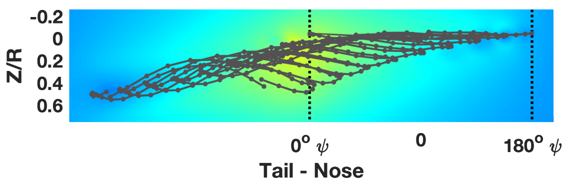

Figure 14. Wake Structure with SSFVW Model at 35 m/s Forward Flight with 5 m/s Climb Trim

14), the wake is deflected downward and elongated, spreading the induced velocity field farther below the rotor. In descent (Figure 15), the wake is redirected upward, resulting in a concentrated region of high induced velocity near the rear of the disc around $\psi = 0°$.

Steady-State Analyses

Steady-state analyses are performed by fixing the control inputs by setting the lateral and longitudinal cyclic to zero and the collective pitch to approximately 8°. The rotor is then subjected to horizontal flow from the nose direction ($\psi = 0°$) with varying wind speeds. Unlike the trim analyses, this setup allows for a direct evaluation of how different inflow models react to external flow conditions. This setup enables a comparative study of the behavior of the inflow models without the influence of any control inputs.

Figure 16 illustrates the flap response of the rotor, highlighting the classical blowback effect with increasing forward velocity. As expected, the coning angle β_0 increases due to greater dynamic pressure. All models follow the same general trend, although the SSFVW model exhibits slightly more nonlinearity in the 20–30 m/s range, where wake distortion becomes more prominent.

The longitudinal flapping angle β_{1c} shows close agreement between the Pitt–Peters and Glauert models up to approximately 30 m/s. Beyond this point, Glauert's skewed wake approximation begins to diverge, while SSFVW predicts about 0.5° greater blowback due to its more accurate wake resolution.

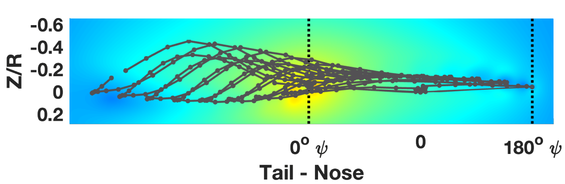

Figure 15. Wake Structure with SSFVW Model at 35 m/s Forward Flight with 5 m/s Descent Trim

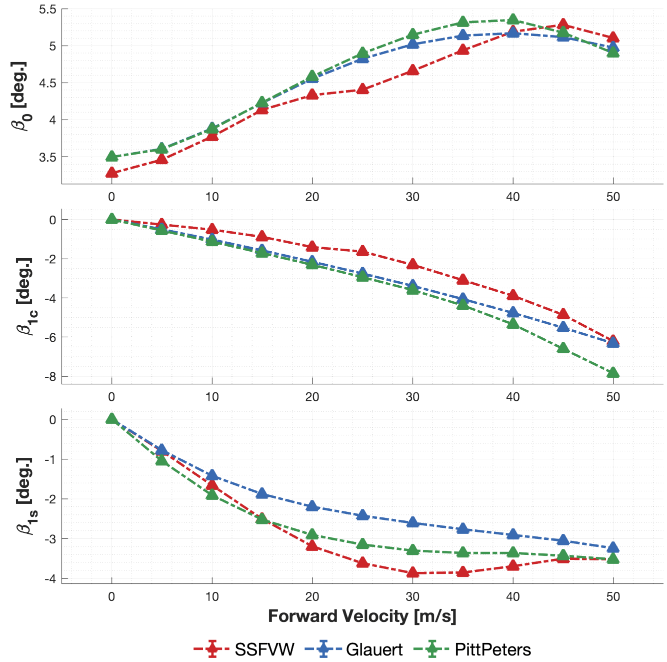

Figure 16. Steady State Flap Angles for Forward Wind

The most pronounced differences occur in the lateral flapping angle β_{1s}. The SSFVW model predicts values up to 1° higher than the analytical models. This discrepancy reflects the improved estimation of in-plane aerodynamic forces by SSFVW, particularly on the advancing side of the rotor, where lateral dynamics are dominant.

Figure 17 presents the vertical force, torque, and hub moments under the same forward flow conditions generated by the rotor. The SSFVW model initially predicts lower vertical force and torque up to around 25 m/s, indicating a slight reduction in rotor efficiency. Between 25 and 40 m/s, the torque increases while vertical force decreases, suggesting a significant loss in aerodynamic efficiency. Beyond 40 m/s, both the Pitt–Peters and SSFVW models exhibit more oscillatory torque and similar behavior, likely due to their sensitivity to wake distortions and unsteady aerodynamic effects.

Simulation Analyses: Gust Response

The purpose of these analyses is to evaluate the dynamic response of each inflow model to transient, non-uniform flight conditions, providing insight into the models' ability to capture unsteady aerodynamic phenomena.

Simulations are initialized from two trimmed conditions: hover and forward flight at 35 m/s. A sinusoidal gust disturbance is introduced, originating from $\psi = 45°$, thereby exciting both longitudinal and lateral axes. The headwind, crosswind, and vertical wind components of the applied gust are shown in Figure 18.

Firstly, in the forward flight case, all three models give similar responses for the given gust as seen in the Figure 19. Especially, the Pitt-Peters and SSFVW methods have very similar responses. In all the cases, the magnitude and phase of the

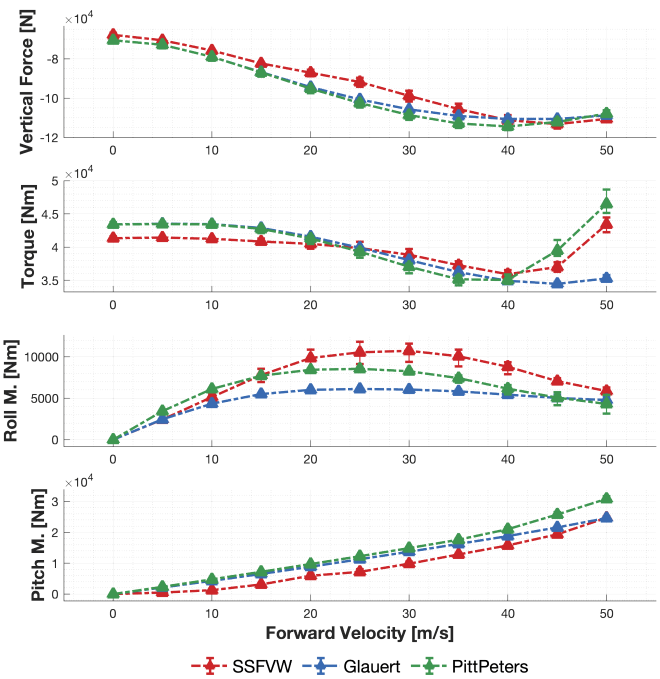

Figure 17. Steady State Forces and Moments for Forward Wind

Glauert model results fall behind the other models because it assumes the analytical solution for that time instant for steady conditions. Another observation from this figure is the amplitude of oscillations, especially the n-per-rev ones. In forward flight, it is expected to have n-per-rev oscillations because of the flap dynamics. However, the Glauert and Pitt-Peters models fail to catch the same frequency oscillations for inflow dynamics that the SSFVW method catches. Hence, the n-per-rev oscillations are much more evident for SSFVW results.

On the other hand, in hover, as seen on Figure 20, the behavior of these models separates. In torque, the Glauert and Pitt-Peters models have similar behavior with a small phase difference, but the SSFVW does not show such a sinusoidal oscillation. It has a similar frequency, but it stays in the peaks a bit, which mirrors the delay from the development of the wake. In moments, the results of the SSFVW and Pitt-Peters are similar to the forward flight case, but the Glauert model gives untraceable and unrealistic results. The reason for these kinds of results from the Glauert model is that it uses different equations for hover and forward flight, and while transitioning, it loses the information about the step before and assumes there is a steady condition at that time instant. Hence, it can be said that the Glauert inflow model is not reliable for transient analysis.

Performance of the Models

In order to measure the computational performance of the inflow models, 60-second simulations are performed using the MATLAB Simulink interface without any code generation. During these simulations, the real-time ratio is computed for each time step by dividing the elapsed computation time by the time step size. The median of these ratios over the full

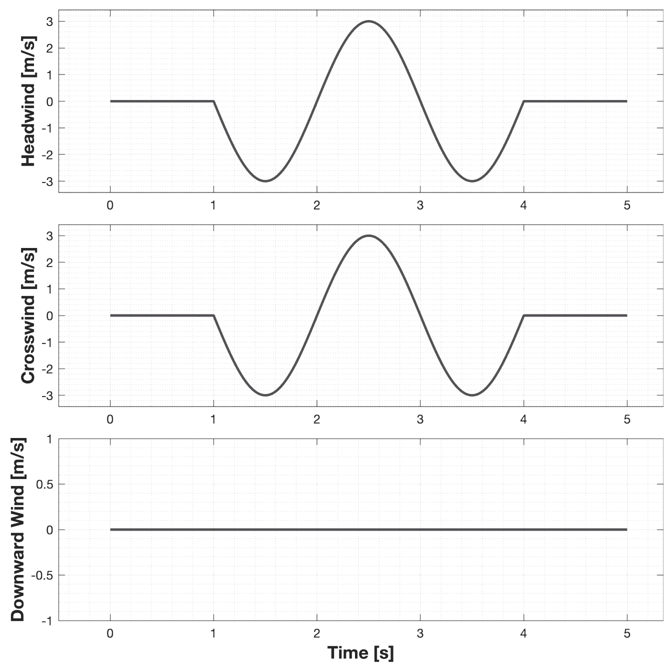

Figure 18. Wind Input for Gust Response Simulations

Table 2. Computational Performance Comparison.

Model	Mean Real-Time Ratio
Glauert	0.14
Pitt-Peters	0.15
SSFVW	8.65

simulation duration is taken as the representative performance metric. This approach provides a consistent basis for comparing the computational efficiency of different inflow models.

As shown in Table 2, both the Glauert and Pitt-Peters inflow models perform significantly faster than real-time, with real-time ratios well below 1. These models are computationally lightweight due to their closed-form or low-order dynamic formulations, making them suitable for applications requiring rapid evaluations such as optimization loops or real-time simulation environments.

In contrast, the SSFVW model exhibits a median real-time ratio of 8.65, indicating that it requires more than eight times the simulation duration in wall-clock time. This increase in computational cost stems from the need to track and convect discrete vortex particles, evaluate induced velocities via the Biot–Savart law, and manage a growing set of wake elements over time. While SSFVW offers the highest fidelity and enables unsteady wake modeling, this computational burden limits its direct applicability in time-critical scenarios.

Despite its high computational cost, the SSFVW model remains an strong tool for high-fidelity off-line analyses, validation efforts, and design evaluations where accurate prediction of unsteady wake dynamics is critical. While the current implementation is not optimized for execution speed, there is a room for improvement through techniques such as code generation, algorithmic optimization, parallel computing, or GPU acceleration. These improvements have the potential to

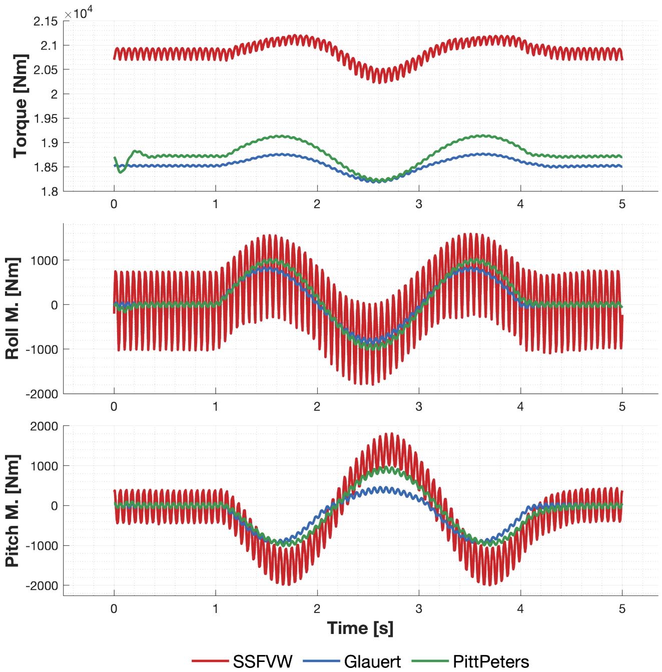

Figure 19. Gust Response Forces and Moments for Forward Flight

significantly reduce computational burden and bring the SSFVW model closer to real-time applicability. With these advancements, the SSFVW approach shows strong promise for future use in advanced simulation platforms.

CONCLUSIONS

This study compared three inflow models; Glauert, Pitt–Peters, and State-Space Free Vortex Wake (SSFVW), using a blade element-based helicopter rotor simulation framework implemented in MATLAB/Simulink.

Overall, the Glauert and Pitt–Peters models demonstrated sufficient accuracy for predicting general trends in steady and trimmed conditions. Their simplicity and computational efficiency make them suitable for rapid analyses, preliminary design iterations, and controller prototyping. However, both models showed limitations in transient simulations.

In contrast, the SSFVW model produced more realistic and detailed results, especially in unsteady cases. It captured the expected n-per-rev oscillations and reflected the wake memory effect in gust response more accurately than the other models. Moreover, it provided better agreement in flap deflections and induced velocity distributions compared to validated benchmarks.

- The SSFVW model offered significantly higher fidelity in dynamic conditions, particularly in gust response and flap dynamics, making it a superior choice for transient simulations.
- Despite its accuracy, SSFVW required a real-time computation ratio of 8.65, limiting its practicality for real-time applications in its current form.

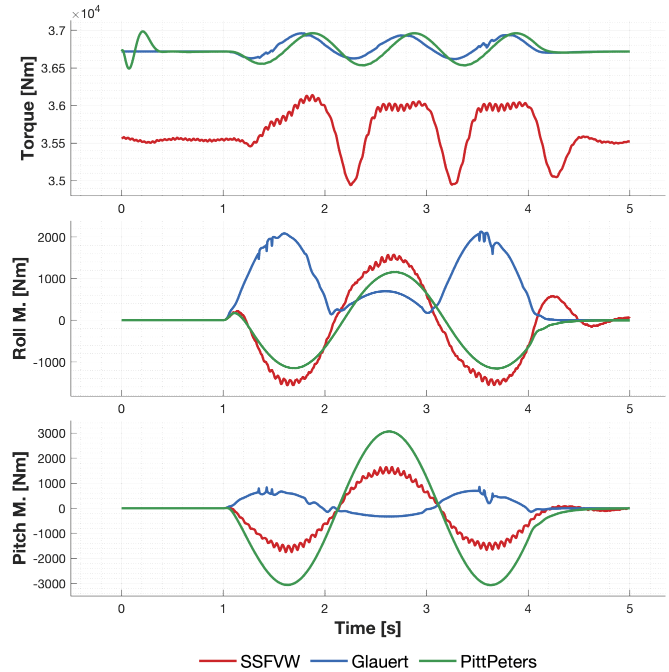

Figure 20. Gust Response Forces and Moments for Hover

Future improvements such as code generation, parallelization, and GPU acceleration may significantly reduce its computational burden. These enhancements could unlock the potential of SSFVW for real-time simulation, hardware-in-the-loop setups, and advanced control system development.

Author contact:
Yusuf Bayrak – yusufbayrak5838@gmail.com
Nilay Sezer Uzol – nuzol@metu.edu.tr

ACKNOWLEDGMENTS

This study is an extension of the author's master's thesis conducted at Middle East Technical University. The authors gratefully acknowledge the support of Turkish Aerospace Industries (TUSAŞ), particularly for providing access to the FlightLab simulation environment under license.

REFERENCES

1. H. Glauert. A general theory of the autogyro. Technical Report ARC RM 1111, Aeronautical Research Council, 1951.
2. D.M. Pitt and L.L. Peters Jr. Theoretical prediction of dynamic inflow derivatives. *Vertica*, 5(1):21–34, 1981.
3. J. Gordon Leishman. *Principles of Helicopter Aerodynamics*. Cambridge University Press, 2000.
4. Wayne Johnson. *Rotorcraft Aeromechanics*. Cambridge Aerospace Series. Cambridge University Press, Cambridge, electronic resource edition, 2013.
5. Gareth D. Padfield. *Helicopter Flight Dynamics: The Theory and Application of Flying Qualities and Simulation Modelling*. AIAA Education Series, 2nd edition, 2007.

6. Inc. Advanced Rotorcraft Technology. Flightlab rotorcraft modeling and simulation software, 2024.

7. Roberto Celi. State-space representation of vortex wakes by the method of lines. *Journal of the American Helicopter Society*, 2005.

8. Diego Hidalgo López. Assessment of a state-space free wake model for rotorcraft flight mechanics applications. Master's thesis, Delft University of Technology, 2014.

9. Umberto Saetti and Joseph F. Horn. Implementation and linearization of a rotor simulation with a state-space free-vortex wake model. *Vertical Flight Society Forum 78*, 2022.

10. Bayrak Yusuf, Dağalp Alper, Boynukalın Muhammet, Uzol Sezer Nilay, Esmek Ceren Cansu, and Okcu Ilgaz Doğa. Development and validation of a blade element model in simulink for rotary wing flight mechanics applications. *12th Ankara International Aerospace Conference*, 2023.

11. Joseph Katz and Allen Plotkin. *Low-Speed Aerodynamics*. Cambridge University Press, 2nd edition, 2001.

CLASSIFICATION & COPYRIGHT